Indian Journal of Chemical Technology
Vol. 29, September 2022, pp. 578-582
DOI: 10.56042/ijct.v2925.61511

Investigation of structural and optical characteristics of CuO nanoparticles calcinated at various temperatures

Smriti Sihag[1], Rita Dahiya[1], Suman Rani[1], Anushree[2], Ashvani Kumar[3] & Vinay Kumar*[,1]

[1]Department of Physics, COBS & H, CCS Haryana Agricultural University, Hisar 125 004, India

[2]Department of Chemistry, COBS & H CCS Haryana Agricultural University, Hisar 125 004, India

[3]Nanoscience Laboratory, Institute Instrumentation Centre, Indian Institute of Technology, Roorkee 247 667, India

E-mail: vinay23@hau.ac.in

Received 16 March 2022; accepted 24 June 2022

Copper oxide nanoparticles (CuO) have been synthesized by utilizing a precipitation approach with copper nitrate ($Cu(NO_3)_2.3H_2O$) as a precursor and sodium hydroxide as a stabilizing agent at different calcination temperatures i.e. 400, 600, and 800°C. X-ray diffraction (XRD), scanning electron microscopy (SEM), Fourier Transform Infrared Spectroscopy (FTIR), UV-Visible spectroscopy (UV-Vis), and photoluminescence spectroscopy (PL) were used to look at the sample's different characteristics. The XRD analysis show that copper oxide nanoparticles have a monoclinic structure with crystallite sizes increasing with increasing calcination temperature up to 600°C, then decreased at 800°C. Also, with increasing temperature, XRD peaks were observed to become sharper, indicating better crystallinity of the samples. FE-SEM image show that synthesized CuO exhibit a flake-like structure, but on calcination it attained a regular particle like structure. The band gap of the material increased as the crystallite size of the material decreased. Photoluminescence intensity was observed to increase with temperature up-to 600°C and then decreased at 800°C. The temperature at which copper oxide nanoparticles were calcined demonstrated to have a considerable impact on their structural and optical properties. The synthesized copper oxide nanoparticles may be employed in the field of electronics in making transistors, heterojunctions, diodes etc. in optoelectronics devices like solar cells, light emitting diodes and in environmental protection for developing gas sensors.

Keywords: Band gap, Calcination, Copper oxide, Optical properties, XRD

Due to the tune-able characteristics of diverse materials at the nano-scale level, there has been a tremendous interest of scientists in the field of nano-science and nanotechnology in the previous few decades[1]. Due to their high specific surface area and surface-to-volume ratio, nano-sized materials have unique and improved chemical, physical, optical, magnetic and mechanical characteristics when compared to their bulk counterparts[2]. Of the various types of nano-materials; metal-oxide are being studied extensively due to their small size, low cost, environment friendliness and chemical stability. Among transition metal oxides, copper oxide nano-materials are of peculiar use as they are p-type semiconductor with holes as the majority carrier. Copper oxide has a monoclinic structure and two phases: cupric oxide and cuprous oxide, both have a direct and narrow bandgap[3]. Due to its suitable band gap along with excellent optical and electrical properties, copper oxide is becoming popular in the field of photovolatics[4]. On exposure to different gases copper oxide shows a change in resistance, so it is widely used as a sensing material in gas sensors[6], It is also being widely used in Li ion batteries[5], optoelectronic device systems[7], thermal conductivity[8], field emission emitter[9], photocatalytic activity[10], biomedical applications[11], environmental applications[12], electrochemical sensor[13] and in the study of antibacterial properties[14]. So, great efforts have been done in recent years in order to prepare copper oxide nano-structures. Hydrothermal[15], sol gel method[16], precipitation method[17], sono-chemical[18], microwave assisted methods[19], solvo-thermal[20], reflux method[21] and electrospinning method[22] are some of the ways that may be utilized to synthesize CuO. The precipitation method, among all of these techniques, is a simple and effective one that has attracted the interest of researchers due to its low energy and temperature requirements, as well as its cost-effective approach for large-scale production and high yield.

Rahnama *et al.* investigated CuO nanoparticles generated by the precipitation method at reaction

temperatures ranging from 10 to 115°C[23]. Phiwdang *et al.* reported the precipitation-based synthesis of copper oxide nanoparticles from various precursors[17]. Investigation of the antibacterial characteristics of copper oxide nanoparticles was done by Ruda *et al.* by adjusting the calcination temperature up to 400°C and using different solvents[24]. Siddiqui *et al.* synthesized different morphologies of copper oxide by changing the copper precursor and studied the various properties of the obtained shapes[25]. An investigation of the influence of different solvents on the optical properties of copper oxide nanoparticles obtained was done by *Horti et al*.[26]. A *p*H based study was done by Chopra *et al.* by varying the amount of oxidizing agent in the copper precursor[27]. Syarif *et al.* produced the nanoparticles of CuO from a chloride precursor and studied their absorption properties for methylene blue after calcination in a temperature range of 300 to 500°C[28]. Thamaraiselvi *et al.* studied the photocurrent response of copper oxide nanoparticles developed by the precipitation method and concluded that copper oxide can be a potential candidate for photoelectrochemical applications[29]. However, information on study of optical characteristics of CuO nanoparticles at a high temperature of 800°C is scanty. Therefore, the present study was carried out to explore how the calcination temperature influenced the structural and optical properties of copper oxide nanoparticles made via precipitation method.

Experimental Section

Chemicals

The copper nitrate trihydrate and sodium hydroxide (AR grade) from Sigma Aldrich were used for synthesis of CuO nanoparticles.

Sample preparation

1.0 M copper nitrate and 1.0 M sodium hydroxide solutions were prepared by dissolving 24.16 g copper nitrate and 4 g sodium hydroxide in 100 mL distilled water, respectively. The NaOH solution was added to copper nitrate solution dropwise and slowly while stirring vigorously until black precipitates formed, and then the solution was left undisturbed overnight. The precipitates were washed with distilled water followed by drying in an oven and then calcination at different temperature for four hours. The as synthesized sample was labeled 'A', whereas the sample calcinated at 400°C was labelled 'B', sample calcinated at 600°C was labelled 'C', and sample calcinated at 800°C was labelled 'D'.

Characterization

The crystallinity of all the synthesized samples was determined using the X-ray diffraction method. The various functional groups present in the samples were examined using Fourier transform infrared spectroscopy (FTIR). The morphology of the samples was evaluated with the help of Field Emission Scanning Electron Microscope (FESEM), and their optical characteristics were investigated using UV-Visible spectroscopy and photoluminescence spectroscopy.

Results and Discussions

XRD analysis

XRD analysis of the samples was performed using Rigaku Miniflex-II diffractometer with CuK_{α} radiation of wavelength 1.5406 A° and angle (2θ) varying from 10° to 90°. The XRD diffractograms for samples A, B, C and D are shown in Figure 1. Crystalline peaks at 2θ angles of 32.2^0, 35.6°, 38.7^0, 48.6^0, 53.2^0, 58.2^0, 61.4^0, 66^0 67.8^0, 72.4^0 and 75.1^0, were observed which corresponds to planes (110), (-111), (111), (-202), (020), (202), (-113), (-311), (220), (311) and (004) respectively and representing the monoclinic structure of the CuO samples[30,31]. The intensity of the peak increased as the calcination temperature rises, but the width decreased, implying that the crystallinity of the samples improves with calcination. Debye's Scherer equation was used to compute the crystallite size of the samples. Samples A, B, C and D had crystallite sizes of 11.52, 18.17, 24.37 and 20 nm, respectively as shown in Table 1. The crystallite size continued to grow, as the calcination temperature rises to 600°C, and decreased upon calcination at 800°C. As the calcination temperature rises, grain boundaries change, causing crystallite size to change. For lower calcination temperature there is a tendency of agglomeration and hence crystallite size increases, but at higher

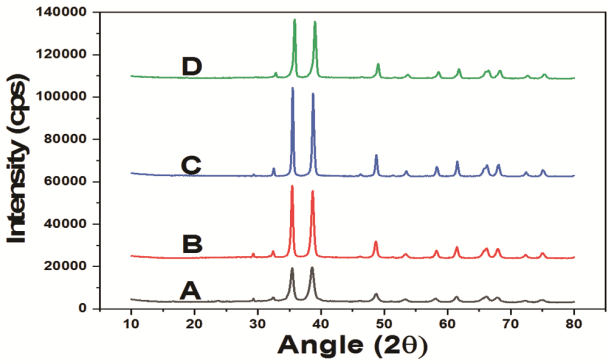

Fig. 1 — XRD graph of samples A, B, C and D.

temperature a decrease in size is observed as particles may break due to heating at such a high temperature[32].

FTIR analysis

A Perkin-Elmer FTIR spectrometer was used to record the FTIR spectra in the range of 4000 cm^{-1} to 400 cm^{-1} in order to examine the different functional groups present in the sample. The FTIR spectrum of samples A, B, C and D are shown in Fig. 2. Peaks at 432, 500, and 610 cm^{-1} is correlated with Cu-O stretching and confirms monoclinic CuO formation [33]. The presence of a peak at 610 cm^{-1} indicates the formation of a Cu-O bond[34]. In sample A, a strong peak around 3500 cm^{-1} was observed which was due to the presence of -OH group. It disappears after calcination of sample as moisture present in the sample must have been vaporized due to heating at high temperature.

Table 1 — Variation of crystallite size and band gap with calcination temperature.

Sample	Calcination temperature (°C)	Crystallite size (nm)	Band gap (eV)
A	As synthesized	11.52	1.5
B	400	18.17	1.47
C	600	24.37	1.42
D	800	20.03	1.48

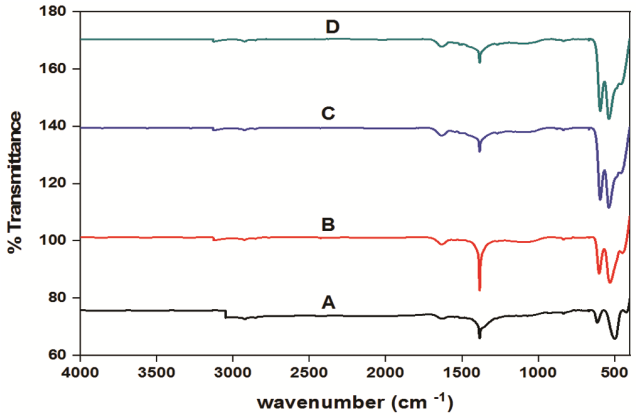

Fig. 2 — FTIR spectra of samples A, B, C and D.

SEM analysis

Study of the morphology of synthesized sample was done using field emission scanning electron microscopy (FE-SEM). FE-SEM images demonstrated that as synthesized sample have a nanoflake-like structure and it turned to particle after calcination at a high temperature (600°C) and crystallinity of the sample got improved. For the increase in calcination temperature upto 600°C there is an increase in agglomeration[35]. With the further increase in temperature to 800°C there are chances for breakage of bonds and hence reduction in crystallite size as evident from Fig. 3.

UV-Visible spectrum

UV-Visible absorption spectra of as synthesized and calcined samples were recorded using an UV-Vis 2600i spectrophotometer as shown in Fig. 4. A red shift in absorption wavelength was observed with the increase in calcination temperature. The band gap of the samples was determined using Tauc's plot as

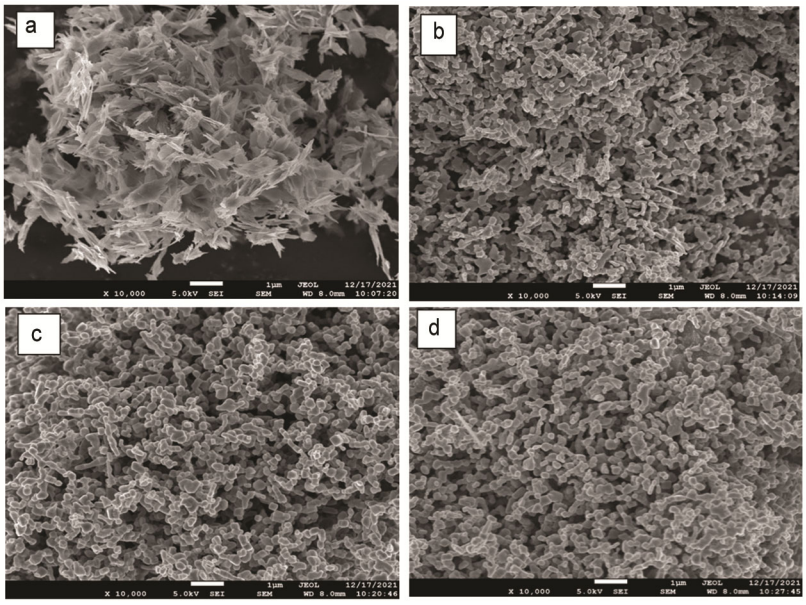

Fig. 3 — FE-SEM image of samples A, B, C and D

shown in Fig. 5. Graph drawn between $(\alpha h\nu)^2$ and hν where intercept of a straight line on x=0 provided the band gap value. The value of the band gap comes out to be 1.5, 1.47, 1.42 and 1.48 eV for sample A, B, C and D respectively, as shown in Table 1. So, with the increase in calcination temperature band gap first decreases and then it starts to increase. It was consistent with the fact that, due to quantum confinement, the value of the band gap increases as particle size decreases[36].

Photoluminescence spectra (PL)

Photoluminescence spectra of all the samples were recorded from Luma 40 spectrophotometer by using excitation radiation of 500 nm as shown in Fig. 6. Emissions were observed at 682, 752 and 822 nm. Peak emission at 682 nm corresponds to near band edge emission[37], emission at 752 nm was due to electron hole recombination at oxygen vacancy and emission at 822 nm was due to bound excitons recombination at a single charged oxygen vacancy[38]. The intensity of the PL signal increases with the increasing calcination temperature up to 600°C, then declines. It could be due to the improved crystallinity and crystallite size of nanoparticles with calcination temperature up to 600°C[39].

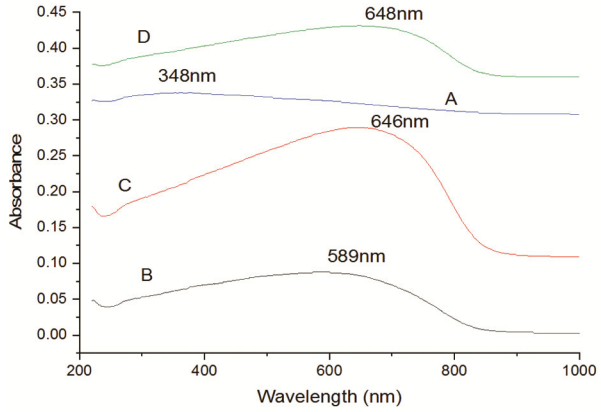

Fig. 4 — UV-Visible absorption spectra of samples A, B, C and D.

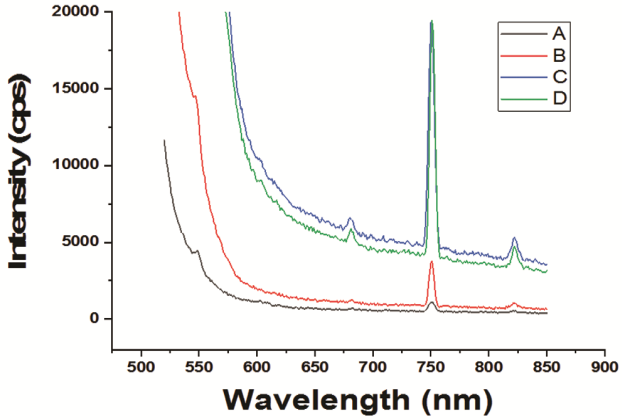

Fig. 6 — Photoluminescence spectra of samples A, B, C and D.

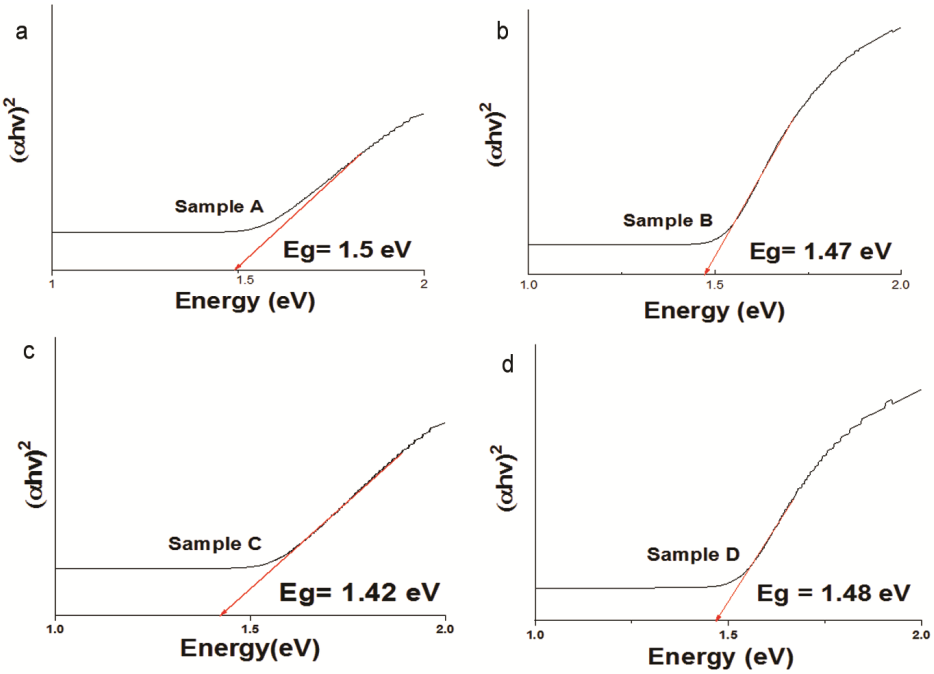

Fig. 5 — Tauc's plot for calculation of the band gap for samples A,B, C and D.

Conclusion

The precipitation approach has been used to make CuO nanoparticles in this study, and their structural and optical characteristics are examined at different values of temperature. XRD result confirm the formation of monoclinic copper oxide and it is observed that with increase in the calcination temperature, crystal size increases up to 600°C, and then it decrease for calcination at 800°C. It was noticed that when the temperature was raised, the crystallinity of the samples improve. FE-SEM images show that regular-sized nanoparticles are formed at high temperatures. The band gap was calculated using the UV-Visible absorption spectrum, and it was discovered that the band gap reduces as the size of nanoparticles increases. It is true in the sense that the band gap rises as particle size decreases owing to quantum confinement. The intensity of the PL signal increases as the crystallinity of the nanoparticles increases with increase in the temperature. Hence it is found that the structural and optical properties of CuO nanoparticles vary strongly with change in calcination temperature and by altering the calcination temperature, we can control the size and band gap of CuO nanoparticles and may utilize the product in numerous applications. Copper oxide nanoparticles obtained in this study can be used in nanotechnology applications like electronics, energy storage devices, optoelectronics, catalytic activity, and sensing.

References

1 Gan Y X, *Nanomaterials Thermoelectric Devices* (Jenny Stanford Publishing), (2018).
2 Khan I, Saeed K & Khan I, *Arab J Chem*, 12 (2019) 908.
3 Akhavan O, Tohidi H & Moshfegh A Z, *Thin Solid Films*, 517 (2009) 6700.
4 Parvathy T, Sabeer N A M, Mohan N & Pradyumnan P P, *Opt Mater (Amst)*, 125 (2022) 112031.
5 Ko S, Lee J, Yang H S, Park S & Jeong U, *Adv Mater*, 24 (2012) 4451.
6 Liu X, Zhang J, Kang Y, Wu S & Wang S, *Cryst Eng Comm*, 14 (2012) 620.
7 Luo L B, Wang X H, Xie C, Li Z J, Lu R, Yang X B & Lu J, *Nanoscale Res Lett*, 9 (2014) 1.
8 Yu W, Zhao J, Wang M, Hu Y, Chen L & Xie H, *Nanoscale Res Lett*, 10 (2015) 1.
9 Erdoğan İ Y & Güllü Ö *J*, *Alloys Compd*, 492 (2010) 378.
10 Aminuzzaman M, Kei L M & Liang W H, *AIP Conference Proceedings*(AIP Publishing LLC), (2017).
11 Verma N & Kumar N, *ACS Biomater Sci Eng*, 5 (2019) 1170.
12 Chandrasekar A, Vasanthraj S, Jagadeesan N L, Shankar S N, Pannerselvem B, Bose V J & Shanmugavel M, *Biocatal Agric Biotechnol*, 33 (2021) 101994.
13 Felix S, Chakkravarthy R B P & Grace A N, *Mater Sci Eng*, 12115 (2015) 147271.
14 Ahmed M H, Javed M T, Bahadur S U K, Tariq A, Tahir M H, Tariq M E, Tariq N, Zarnab S & Ali M H*, Appl Nanosci*, 12 (2022) 2031.
15 Meng D, Liu D, Wang G, San X, Shen Y, Jin Q & Meng F, *Vacuum*, 144 (2017) 272.
16 Mallick P & Sahu S, *Nanosci Nanotechnol*, 2 (2012) 71.
17 Phiwdang K, Suphankij S, Mekprasart W & Pecharapa W, *Energy Procedia*, 34 (2013) 740.
18 Silva N, Ramírez S, Díaz I, Garcia A & Hassan N, *Materials (Basel)*, 12 (2019) 804.
19 Shaalan N M, Rashad M & Abdel-Rahim M A,*Opt Quantum Electron*, 48 (2016) 1.
20 Nogueira A E, Giroto A S, Neto A B S & Ribeiro C, *Colloids Surf A Physicochem Eng Asp*, 498 (2016) 161.
21 Elango M, Deepa M, Subramanian R & Mohamed Musthafa A, *Polym Plast Technol Eng*, 57 (2018) 1440.
22 Khalil A, Jouiad M, Khraisheh M & Hashaikeh R, *J Nanomater*, 2014 (2014) 80.
23 Rahnama A & Gharagozlou M, *Opt Quantum Electron*, 44 (2012) 313.
24 Ruda D A, Ghadhban E & Al-Karam L Q, *AIP Conference Proceedings*, 2372 (2021) 20004.
25 Siddiqui H, Qureshi M S & Haque F Z, *Optik (Stuttg)*, 127 (2016) 4726.
26 Horti N C, Kamatagi M D, Patil N R, Sannaikar M S & Inamdar S R, *J Nanophotonics*, 14 (2020) 46010.
27 Chopra R, Kashyap N Kumar A & Banerjee D, *Int J Eng Res Technol*, 9 (2020) 258.
28 Syarif D, Aliah H, Usman J & Pratiwi Y, *Proceedings 1st Int Conf Islam Sci Technol*, (ICONISTECH) (2019) 11.
29 Thamaraiselvi S & Thenmozhi G, *IJSR*, 11 (2022) 2319.
30 Geetha M P, Pratheeksha P & Subrahmanya B K, *Cogent Eng*,7 (2020) 1783102.
31 Syame S M, Mohamed W S, Mahmoud R K & Omara S T, *Orient J Chem*, 33 (2017) 2959.
32 George A, Raj D M A, Raj A D, Irudayaraj A A, Arumugam J, Prabu H & Kaviyarasu K, *Surf Interf*, 21 (2020) 100761.
33 Ethiraj A S & Kang D J, *Nanoscale Res Lett*, 7 (2012) 1.
34 Bodade A B, Taiwade M A & Chaudhari G N, *J Appl Pharm Res*, 5 (2017) 30.
35 Mahato T H, Singh B, Srivastava A K, Prasad G, Srivastava A R, Ganesan K & Vijayaraghavan R, *J Hazard Mater*, 192 (2011) 1890.
36 Koshy J & George K C, *Int J Nanosci Nanotechnol*, 6 (2015) 1.
37 Aslani A, *Phys B Condens Matter*, 406 (2011) 150.
38 Carranco H, Juarez-Diaz G, Galvan-Arellano M & Martinex-Juarez J*, J Lumin*, 129 (2009) 1483.
39 Toboonsung B & Singjai P, *J Alloys Compd*, 509 (2011) 4132.